CEAS COUNCIL OF EUROPEAN AEROSPACE SOCIETIES

Aerospace Europe
6th CEAS Conference

Optimization of noise abatement aircraft terminal routes using a multi-objective evolutionary algorithm based on decomposition

V. Ho-Huu[1], S. Hartjes[2], L. H. Geijselaers[3], H. G. Visser[4], R. Curran[5]
Faculty of Aerospace Engineering, Delft University of Technology, Delft, The Netherlands
[1]PhD candidate, [2]Asisstant professor, [3]Master student, [4]Associate professor, [5]Professor
Address: P.O. Box 5058, 2600 GB Delft, The Netherlands
E-mails: v.hohuu@tudelft.nl (V. Ho-Huu), s.hartjes@tudelft.nl (S. Hartjes), liset.geijselaers@gmail.com (L. H. Geijselaers) h.g.visser@tudelft.nl (H. G. Visser), r.curran@tudelft.nl (R. Curran)

ABSTRACT

Recently, a multi-objective evolutionary algorithm based on decomposition (MOEA/D) has emerged as a potential method for solving multi-objective optimization problems (MOPs) and attracted much attention from researchers. In MOEA/D, the MOPs are decomposed into a number of scalar optimization sub-problems, and these sub-problems are optimized concurrently by only utilizing the information from their neighboring sub-problems. Thanks to these advantages, MOEA/D has demonstrated to be more efficient than the non-dominated sorting genetic algorithm II (NSGA-II) and other methods. However, its applications to practical problems are still limited, especially in the domain of aerospace engineering. Therefore, this paper aims to present a new application of MOEA/D for the optimal design of noise abatement aircraft terminal routes. First, in order to optimize aircraft noise for aircraft terminal routes while taking into account the interests of various stakeholders, bi-objective optimization problems including noise and fuel consumption are formulated, in which both the ground track and vertical profile of a terminal route are optimized simultaneously. Then, MOEA/D is applied to solve these problems. Furthermore, to ensure the design space of vertical profiles is always feasible during the optimization process, a trajectory parameterization technique recently proposed is also used. This technique aims at reducing the number of model evaluations of MOEA/D and hence the computational cost will decrease significantly. The efficiency and reliability of the developed method are evaluated through case studies for departure and arrival routes at Rotterdam The Hague Airport in the Netherlands.

KEYWORDS: *terminal routes, trajectory optimization, noise abatement, fuel consumption, MOEA/D.*

NOMENCLATURE

D	– Drag force	V_{EAS}	– Equivalent airspeed
ff	– Fuel flow	V_{TAS}	– True airspeed
g_0	– Gravitational acceleration	W	– Aircraft weight
h	– Altitude	γ	– Flight path angle
s	– Along-track distance	ρ	– Ambient air density
T	– Thrust force	ρ_0	– Air density at sea level

1 INTRODUCTION

With the substantial contribution of aviation to the development of business, communication and tourism globally, the air transport industry is expected to grow rapidly in the coming years [1]. However, one of the considerable concerns which policymakers are facing with the extension of aircraft and airport operations is the protest of near-airport communities. This is because of the significant increase in negative impacts on the environment such as noise and pollutant emissions, which directly affect the daily life of communities surrounding airports. Therefore, to grow the air transport sustainably, it is crucial to figure out feasible solutions for decreasing its adverse influences. One of the potential options is the optimal design of new terminal routes (i.e. departure and arrival routes), which has been widely studied during the past few years [2].

Research on optimization of environmentally friendly terminal routes has obtained significant achievements, and different approaches have been proposed in recent years. Hartjes et al. [3] developed a trajectory optimisation tool NOISHHH including a noise model, an emissions inventory model, a geographic information system and a dynamic trajectory optimisation algorithm to generate environmentally optimal departure trajectories based on area navigation. This tool was also used for the optimal design of area navigation noise abatement approach trajectories in [4,5]. Prats et al. [6], [7] applied a lexicographic optimization technique to deal with aircraft departure trajectories for minimizing noise annoyance. Torres et al. [8] proposed a non-gradient optimizer called multi-objective mesh adaptive direct search (multi-MADS) to optimize departure trajectories for NOx emissions and noise at a single measurement point. Recently, Hartjes & Visser [9] employed an elitist non-dominated sorting genetic algorithm (NSGA-II) combined with a novel trajectory parameterization technique for the optimal design of departure trajectories with environmental criteria.

Based on the obtained results from [8,9], it is evident that the use of non-gradient multi-objective optimization methods is one of the efficient approaches for the optimal design of terminal routes. These methods do not only help find out a set of non-dominate optimal solutions, but also help avoid the limitations of gradient methods in coping with discontinuous problems and integer or/and discrete design variables. Up to now, besides multi-MADS and NSGA-II, there are various multi-objective optimization algorithms available in literature, which may also be potential candidates for solving these kinds of problems. However, as yet, they have not been properly investigated. Among them, MOEA/D recently emerged as a powerful method, and has received much attention from researchers. Compared to NSGA-II, MOEA/D is better in terms of both the quality of solutions and the convergence rate [10], which are promising features for solving large-scale real-world problems. Nevertheless, the application of MOEA/D for real engineering problems is still limited, especially in the domain of aerospace engineering. This paper, therefore, aims to apply MOEA/D to the optimization of noise abatement aircraft terminal routes. In order to make the applied algorithm more efficient, advantageous features recently developed for MOEA/D are also integrated into the proposed version. They include an adaptive replacement strategy [11], a stopping condition criterion [12], and a constraint-handling technique [13]. Moreover, to reduce redundant evaluations of infeasible solutions derived from operational constraints during different flight phases, the new trajectory parameterization technique in [9] is also employed. The robustness and reliability of the proposed approach are validated through two numerical examples comprising of a departure route and an arrival route at Rotterdam The Hague Airport.

2 AIRCRAFT MODEL

In this study, an intermediate point-mass model [9] is used. This model relies on several assumptions: 1) there is no wind present, 2) the Earth is flat and non-rotating, 3) the flight is coordinated. Furthermore, the flight path angle is considered sufficiently small ($\gamma < 15^0$). With these assumptions, the equations of motion can be written as:

$$\begin{aligned} \dot{V}_{\mathrm{TAS}} &= g_0 \cdot ((T-D)/W - \sin\gamma) \\ \dot{s} &= V_{\mathrm{TAS}} \cdot \cos\gamma \\ \dot{h} &= V_{\mathrm{TAS}} \cdot \sin\gamma \\ \dot{W} &= -ff \cdot g_0 \end{aligned} \tag{1}$$

where $\dot{V}_{\mathrm{TAS}}, \dot{s}, \dot{h}$ and $\dot{W}$ are the derivatives of true airspeed, distance flown, altitude and aircraft weight, respectively; and *T*, *D*, and *ff* are, respectively, thrust, drag, and fuel flow.

At a condition of low altitude and speed, equivalent airspeed V_{EAS} can serve as a proxy for an indicated airspeed, and can be derived from the true airspeed by the following relationship:

$$V_{\mathrm{EAS}} = V_{\mathrm{TAS}} \cdot \sqrt{\rho/\rho_0} \tag{2}$$

where ρ is the ambient air density, and ρ_0 is the air density at sea level.

By applying Eq. (2), the first equation in Eq. (1) can be rewritten as follows:

$$\dot{V}_{\mathrm{EAS}} = [g_0 \cdot ((T-D)/W - \sin\gamma) + 1/(2\rho) \cdot \mathrm{d}\rho/\mathrm{d}h \cdot V_{\mathrm{TAS}}^2 \cdot \sin\gamma] \cdot \sqrt{\rho/\rho_0} \tag{3}$$

where $\mathrm{d}\rho/\mathrm{d}h$ is the derivative of the ambient air density with respect to altitude.

The aircraft performance model has two control variables, viz. the flight path angle γ and thrust T, and four state variables $\mathbf{x} = [V_{\mathrm{EAS}}\ h\ s\ W]$.

3 TRAJECTORY PARAMETERIZATION

With the effort of reducing the number of model evaluations of infeasible solutions during the optimization process, Hartjes & Visser [9] proposed a novel trajectory parameterization which can diminish significantly the number of operational constraints in the problem formulation. The technique divides a trajectory into two separate parts, a ground track and a vertical path.

For the ground track generation, a modern navigation technology known as required navigation performance (RNP) is employed. In the RNP, track-to-a-fix (TF) and radius-to-a-fix (RF) leg types are often used for constructing a flight path between waypoints. This is because of their abilities in avoiding noise-sensitive areas and minimizing flight track dispersion. By using these two segment types, the ground track can be generated by using only straight legs, and constant radius turns as shown in Figure 1. In this figure, the optimal design variables include L_1, L_2, L_3, R_1, R_2, R_3, $\Delta\chi_1$, and $\Delta\chi_2$, while L_4 and $\Delta\chi_3$ are defined based on geometric relationships.

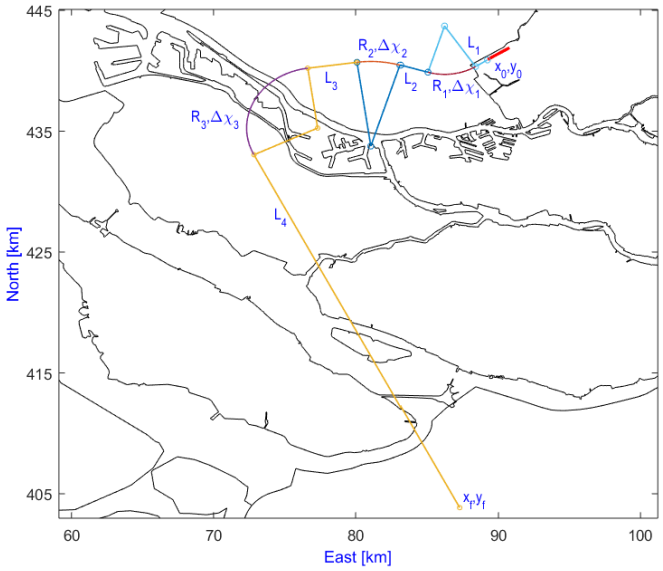

Figure 1. Ground track parameterization.

For the vertical path, the vertical profile is synthesized based on flight procedures derived from ICAO [14]. For instance, aircraft are not allowed to descend and/or decelerate during departure and ascend and/or accelerate during arrival. In order to parameterize this part, the trajectory is split into a number of segments. In each segment, two control inputs (i.e. flight path angle setting $\gamma_{n,i}$ and throttle setting Γ) are kept constant, and they are either directly assigned based on operational requirements or designated as optimal design variables. For each segment, the flight path angle γ_i and thrust T_i are set by adjusting their normalized control optimization parameters $\gamma_{n,i}(0 \leq \gamma_{n,i} \leq 1)$, and $\Gamma_{n,i}(0 \leq \Gamma_{n,i} \leq 1)$, respectively, as follows:

$$\gamma_i = (\gamma_{\max,i} - \gamma_{\min,i})\gamma_{n,i} + \gamma_{\min,i} \tag{4}$$

$$T_i = (T_{\max,i} - T_{\min,i})\Gamma_{n,i} + T_{\min,i} \tag{5}$$

where the subscript n presents a normalized control optimization parameter. The subscripts $\max, i$ and $\min, i$ indicate the maximum and minimum allowable values of the flight path angle and thrust for ith segment, which are specified based on the features of flight procedures.

In the departure procedure, $T_{\max}$ is set to be either maximum take-off thrust (TO) or maximum climb thrust (TCL), depending on the flight stage. In addition, since descending is not permitted in this phase ($\dot{h} \geq 0$), the minimum flight path angle is set to zero ($\gamma_{\min} = 0$). Furthermore, $\gamma_{\max}$ can be defined from the first equation in Eq. (3) based on an assumption that an aircraft is flying with a maximum thrust at a constant speed ($\dot{V}_{\mathrm{EAS}} = 0$). From this equation, $T_{\min}$ can also be determined

when a minimum thrust is required to maintain the aircraft at constant speed ($\dot{V}_{\mathrm{EAS}} = 0$). These formulas are derived as follows:

$$\gamma_{\max} = \sin^{-1}[(-2 \cdot \rho \cdot g_0 \cdot (T_{\max} - D))/(W(\mathrm{d}\rho/\mathrm{d}h \cdot V_{\mathrm{TAS}}^2 - 2 \cdot \rho \cdot g_0))] \cdot \quad (6)$$

$$T_{\min} = D - (W/(2 \cdot \rho \cdot g_0) \cdot \mathrm{d}\rho/\mathrm{d}h \cdot V_{\mathrm{TAS}}^2 \cdot \sin\gamma) + W \cdot \sin\gamma \quad (7)$$

In the arrival procedure, the minimum thrust $T_{\min}$, called an idle thrust is derived for each specific aircraft model, whilst the maximum flight path angle is set to zero ($\gamma_{\max} = 0$) because ascending is not allowed in this phase ($\dot{h} \leq 0$). In addition, by assuming that the aircraft can only maintain its speed during descending when the maximum thrust is applied, $T_{\max}$ can be determined by the same formula in Eq. (7) with a replacement of $T_{\min}$ by $T_{\max}$. The minimum flight path angle $\gamma_{\min}$ is evaluated with respect to the minimum thrust $T_{\min}$ by the same formula in Eq. (6) with a replacement of $T_{\max}$ and $\gamma_{\max}$ by $T_{\min}$ and $\gamma_{\min}$.

4 PROBLEM STATEMENT

The aim of the study is to optimally design terminal routes which can help to reduce the negative impact of aircraft noise in near-airport communities. However, purely focussing on noise impact may lead to a considerable increase in fuel consumption which is against the interests of stakeholders like airline companies. To take into account this issue, two conflicting objectives (one related to noise and the other related to fuel consumption) are therefore considered in this study.

While the fuel consumption can easily be measured by the change of the aircraft weight from Eq. (1), noise impact is more difficult to quantify. To assess the influence of aircraft noise on near-airport communities, the percentage of people who are likely to be awakened due to aircraft noise exposure is employed in this paper. This criterion was proposed by the Federal Interagency Committee on Aviation Noise (FICAN) in 1997 and defined as follows [15]:

$$\%Awakening = 0.0087 \cdot (SEL_{\mathrm{indoor}} - 30)^{1.79} \quad (8)$$

where $\%Awakening$ is the maximum percentage of awakened people owing to noise of an aircraft. SEL_{indoor} is the indoor sound exposure level (dBA) and is evaluated by using a replica of the integrated noise model (INM) [9]. Because *SEL* calculated from INM represents an outdoor value, an amount of 20.5 dB is subtracted to obtain SEL_{indoor}, accounting for the sound absorption of an average house [2].

With the above definitions of two objectives, the optimization problem is formulated as follows:

$$\begin{aligned} &\min_{\mathbf{x},\boldsymbol{\gamma}_n,\boldsymbol{\Gamma}_n} && \{number\ of\ awakening, fuel\ burn\} \\ &\text{s.t.} && h = h_{\mathrm{final}}, \quad V_{\mathrm{EAS}} = V_{\mathrm{EAS\_final}} \end{aligned} \quad (9)$$

where $\mathbf{x}$ is the vector of ground track variables. $\boldsymbol{\gamma}_n$ and $\boldsymbol{\Gamma}_n$ are the vectors of the flight path angle setting and throttle setting variables on segments. The parameters h_{final} and $V_{\mathrm{EAS\_final}}$ are, respectively, the final altitude and equivalent airspeed of the flight procedures.

5 MOEA/D ALGORITHM

Many real-world problems present themselves as complex optimization problems with more than two conflicting objectives and this has given rise to the birth of various multi-objective optimization methods. Among the various different algorithms, the MOEA/D method, firstly developed by Zhang & Li [16], has been emerged as a promising, potential method for solving complicated multi-objective optimization problems (MOPs) [17]. In MOEA/D, the MOPs are transformed into a set of single optimization sub-problems by applying decomposition approaches, and then evolutionary optimization methods are applied to optimize these sub-problems simultaneously. In recent years, MOEA/D has been applied in different fields such as power system transmission and distribution networks [18], and wireless sensor networks [19]; and various versions have been developed such as MOEA/D-DE [10], MOEA/D-DRA [20], and MOEA/D-GR [11]. Although there are many variants of MOEA/D available in literature, a powerful single version of MOEA/D that combines different advantages of current versions is not yet in place. With the aim of developing an efficient algorithm for the presented problem, therefore, an MOEA/D version which is the combination of MOEA/D-DE [10] with an adaptive replacement strategy [11], a stopping condition criterion [12] and a constraint-handling

technique [13] is developed in this study. The general framework of the algorithm is presented in Algorithm 1. For more detail, readers are encouraged to refer to Refs. [10–13]

Algorithm 1. Pseudo-code of MOEA/D algorithm

Input:

- A multi-objective optimization problem as Eq. (9);
- A stopping criterion;
- N: number of sub-problems;
- $\mathbf{w}^i = (w_1^i, .., w_m^i), i = 1, \dots, N$**:** a set of N weight vectors;
- T_m: size of mating neighbourhood;
- $T_{r\max}$: maximum size of replacement neighbourhood;
- δ: the probability that mating parents are selected from the neighbourhood;
- *MaxIter*: maximum iteration;
- *FEs* = 0: the number of function evaluations;

Step 1. Initialization

1.1. Find the T_m closest weight vectors to each weight vector based on the Euclidean distances of any two weight vectors. For each sub-problem $i = 1, \dots, N$ set $\mathbf{B}^i = (i_1, .., i_{T_m})$ where $\mathbf{w}^{i_1}, \dots, \mathbf{w}^{i_{T_m}}$ are the closest weight vectors to $\mathbf{w}^i$;

1.2. Create an initial population $\mathbf{P} = \{\mathbf{x}^i, \dots, \mathbf{x}^N\}$ by uniformly randomly sampling from design space Ω. Evaluate the fitness value FV^i of each solution $\mathbf{x}^i$, i.e. $FV^i = \left(f_1(\mathbf{x}^i), \dots, f_m(\mathbf{x}^i)\right)$ and set $\mathbf{FV} = \{FV^1(\mathbf{x}^1), \dots, FV^N(\mathbf{x}^N)\}$;

1.3. Initialize ideal point $\mathbf{z}^* = (z_1^*, \dots, z_m^*)^{\mathrm{T}}$ by setting $z_j^* = \min\{f_j(\mathbf{x}) | \mathbf{x} \in \Omega,\ j = 1, .., m\}^{\mathrm{T}}$and nadir point $\mathbf{z}^{\mathrm{nad}} = (z_1^{\mathrm{nad}}, \dots, z_m^{\mathrm{nad}})^{\mathrm{T}}$ by setting $z_j^* = \max\{f_j(\mathbf{x}) | \mathbf{x} \in \Omega,\ j = 1, .., m\}^{\mathrm{T}}$;

1.4. Set *FEs* = *FEs* + N, and generation: *gen* = 1;

Step 2. Update

while (the stopping condition is not satisfied)

for $i = 1, \dots, N$; do

2.1. Selection of mating/update range

Set $\mathbf{B}_m = \begin{cases} \mathbf{B}^i & if\ rand < \delta \\ \{1, \dots, N\} & \text{otherwise} \end{cases}$

where *rand* is a uniformly distributed random number in [0,1];

2.2. Reproduction: randomly select three parent individuals r_1, r_2 and r_3 $(r_1 \neq r_2 \neq r_3 \neq i)$ from $\mathbf{B}_m$ and generate a solution $\bar{\mathbf{y}}$ by applying "DE/rand/1" operator, and then perform a mutation operator on $\bar{\mathbf{y}}$ to create a new solution $\mathbf{y}$;

2.3. Repair: if any element of $\mathbf{y}$ is out of Ω, its value will be randomly regenerated inside Ω;

2.4. Evaluate the fitness value of new solution $\mathbf{y}$;

2.5. Update of $\mathbf{z}^*$ and $\mathbf{z}^{\mathrm{nad}}$: for each j = 1,..., m if $z_j^* \leq f_j(\mathbf{x}^i)$ then set $z_j^* = f_j(\mathbf{x}^i)$**,** and if $z_j^{\mathrm{nad}} \geq f_j(\mathbf{x}^i)$ then set $z_j^{\mathrm{nad}} = f_j(\mathbf{x}^i)$;

2.6. Update of solutions: use an adaptive replacement strategy in [11]:

end for

Set *FEs* = *FEs* + N, and *gen* = *gen* + 1;

Step 3. Stopping condition

Use a stopping criterion in [12].

if (stopping criterion is satisfied or *MaxIter* is reached)

Stop the algorithm;

end if

end while

Output: Pareto set $\mathbf{PS} = \{\mathbf{x}^1, \dots, \mathbf{x}^N\}$; Pareto front $\mathbf{PF} = \{FV^1(\mathbf{x}^1), \dots, FV^1(\mathbf{x}^N)\}$.

6 NUMERICAL EXAMPLE

To evaluate the applicability and effectiveness of MOEA/D for dealing with optimization of noise abatement terminal routes, two scenarios including departure and arrival at Rotterdam The Hague Airport are considered in this section. The airport is located in the north of Rotterdam city, the Netherlands, and is surrounded by densely populated regions such as The Hague, Rotterdam, and Utrecht. It has one runway which can be operated in both directions, labelled as 06 and 24. The investigated cases include a standard instrument departure (SID) named WOODY1B starting from runway 24 and finishing at waypoint EH162, and a standard terminal arrival route (STAR) named STD starting at a ground based beacon STD and finishing at way point EH252 as shown in Figure 2. The population density data with a grid size of 500m×500m taken from [21] is utilised and illustrated in

Figure 2 as well. An aircraft model of a Boeing 737 with twin engines is used. To compare the performance of MOEA/D, the well-known NSGA-II [22] is also applied to solve these problems. A population size of 50 is used for both methods, and the algorithms will stop when either their convergence criteria are satisfied, or the maximum number of iterations (*MaxIter*) is reached, where *MaxIter* is set to 1000. All algorithms are implemented in Matlab 2016b on a Core i7, 8GB ram laptop.

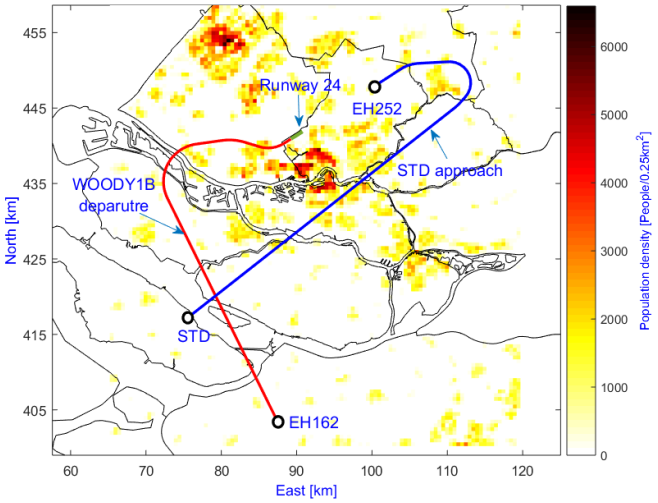

Figure 2. Departure and arrival scenarios.

6.1 Departure route

The simulation of this problem is started at an altitude of 35 ft and a take-off safety speed V_2 + 10 kts with the landing gear retracted and departure flaps selected, and is terminated at an altitude of 6,000 ft and an equivalent airspeed (EAS) of 250 kts. The ground track is constructed by four straight legs and three turns as shown in Figure 1, while the vertical path is subdivided into 10 segments. The vertical profile parameters including both the optimal and reference cases are derived from [9].

The Pareto-optimal solutions obtained by the methods are shown in Figure 3, and their corresponding ground tracks are illustrated in Figure 4. From a perspective of solution methods, it can be seen from Figure 3 that MOEA/D gives more dominating solutions of awakening, whilst NSGA-II has more solutions regarding fuel burn. In general, however, it can be observed that MOEA/D is better than NSGA-II. Moreover, to get these results, MOEA/D only requires 39,371 model evaluations in 6.45 hours, whilst NSGA-II required 50,000 evaluations in 8.17 hours. From an engineering point of view, it can be observed that the obtained ground tracks in Figure 4 appear to be reasonable and appropriate. There are four different groups of ground tracks obtained by MOEA/D and three groups obtained by NSGA-II, and all of them try to avoid densely populated regions. This helps to explain why there are some gaps on the Pareto fronts. Compared to the reference case, all solutions feature a shorter ground track and better environmental performance.

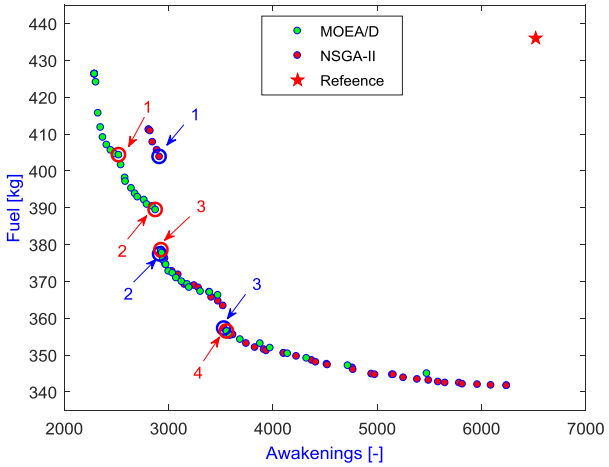

Figure 3. Comparison of Pareto-optimal solutions obtained by NSGA-II and MOEA/D and the result of the reference case.

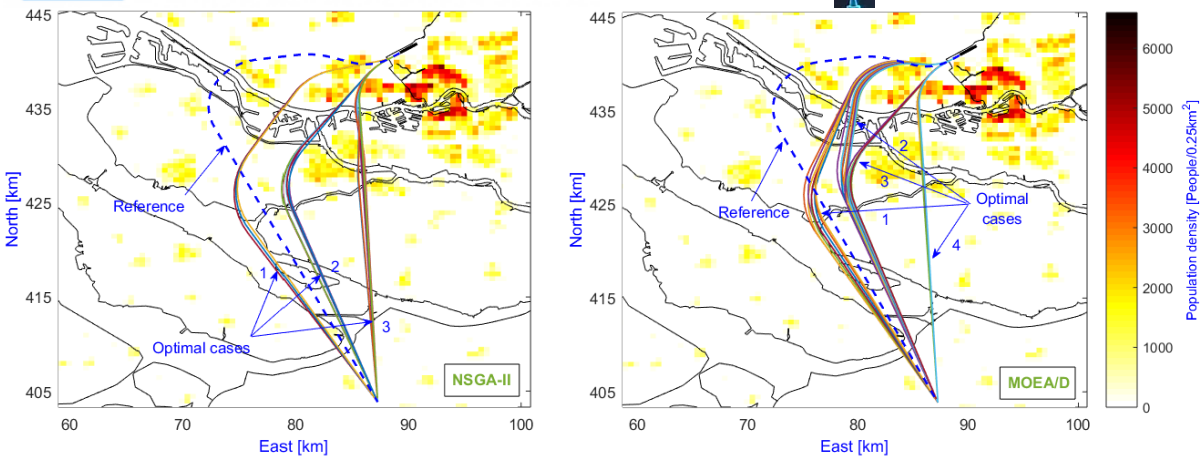

Figure 4. Optimal ground tracks obtained by NSGA-II and MOEA/D.

For a comparison of performances, the expected number of awakenings and fuel burn of four representative cases extracted from the Pareto fronts (numbered as shown in Figure 2) and those of the reference case are presented in Table 1. Their corresponding vertical profiles are also given in Figure 5. It is seen from the table that all optimal cases give a better solution for time, fuel and awakenings. It is also observed that the cases with shorter routes (i.e. 2 and 3) have less fuel burn but more awakenings, which are the results of directly flying over areas with dense population. When looking at the vertical profiles in Figure 5, it is indicated that all four optimal cases prefer a low altitude, which is because the spread of aircraft noise at a low altitude is smaller than that at a higher altitude due to increased lateral attenuation; and hence it may lead to a significant reduction of awakenings. For the airspeed shapes, there are some distinct levels which may be due to either the constraints of a bank angle or reducing thrust when flying over populated areas.

Table 1. Comparison of objectives of cases 1-4 and the reference case.

Case number		Time (s)	Fuel (kg)	Awakening
Reference		420.90	436.02	6519
1	MOEA/D	383.40	404.28	2523
	NSGA-II	385.29	403.80	2912
2	MOEA/D	360.46	389.39	2875
	NSGA-II	343.33	377.31	2918
3	MOEA/D	344.38	378.47	2930
	NSGA-II	311.07	357.19	3532
4	MOEA/D	308.60	356.39	3558

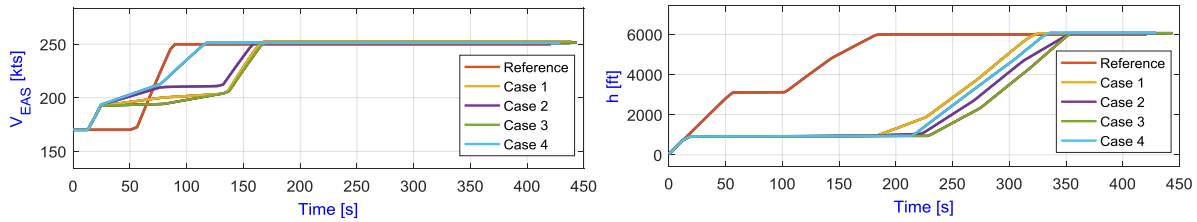

Figure 5. Vertical profiles of cases 1-4 and the reference case.

Although the obtained solutions are better than the reference case, from a practical perspective, they may not be accepted in reality because of flying at a low altitude for a long time. Thus, to make optimal solutions more applicable, an additional constraint on the flight path angle is applied, where the normalized control parameter $\gamma_{n,i}$ is set to be larger than 0.2 from an altitude of 35 ft to 1,500 ft i.e. if h $\leq$ 1,500 ft, $(0.2 \leq \gamma_{n,i} \leq 1)$, otherwise $(0 \leq \gamma_{n,i} \leq 1)$. With this new constraint, the optimal results obtained by MOEA/D are given in Figure 6a in relation to the previous situation, their ground tracks are provided in Figure 6b, and the vertical profiles of two representative cases (1 and 4) are indicated in Figure 7. It can be observed that all new solutions have larger values for the objectives, especially in the number of awakenings which can be due to increasing the dispersion of aircraft noise at a higher altitude. This may also be the cause of slight changes in the ground tracks. The shapes of the airspeed and altitude histories have not changed much, except for an increase in altitude.

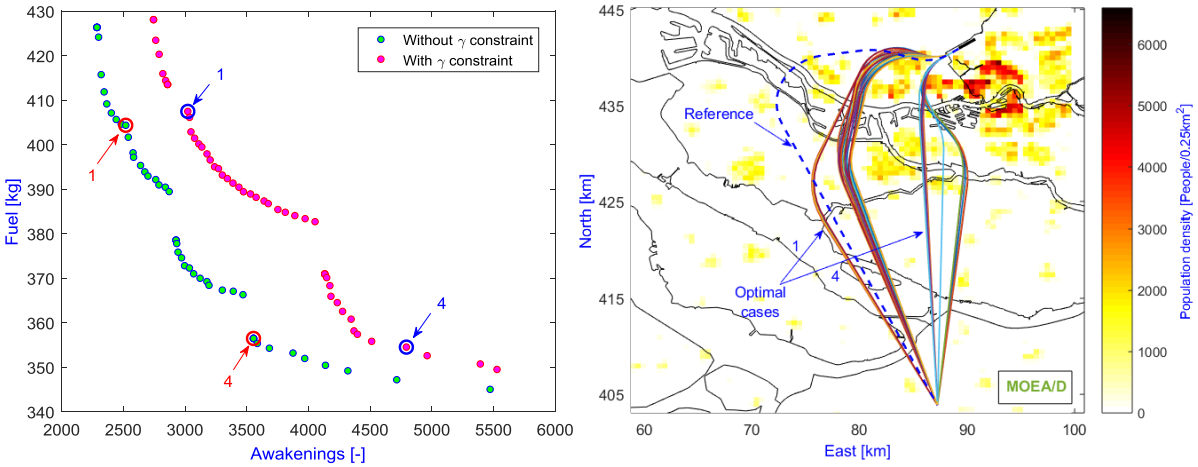

Figure 6. a) Optimal objectives with and without the new constraint of $\gamma_{i,n}$; b) Optimal ground tracks.

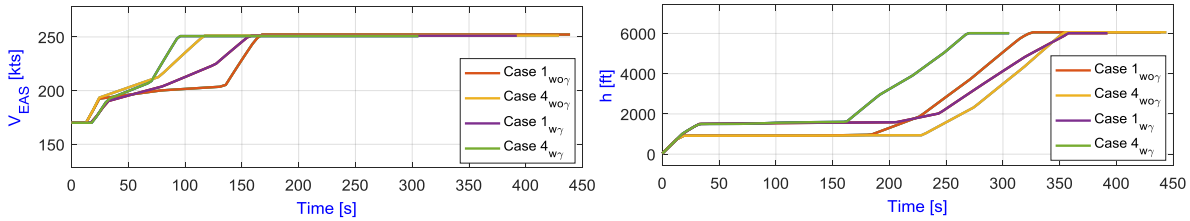

Figure 7. Comparison of vertical profiles of cases 1 and 4 with and without the new constraint of $\gamma_{n,i}$.

6.2 Arrival route

For this problem, the simulation is started at an altitude of 6,000 ft and an equivalent airspeed of 250 kts, and is finished at an altitude of 2,000 ft and an equivalent airspeed of 170 kts. Similar to the departure problem, the ground track is also constructed by four straight legs and three turns, and the vertical path is also subdivided into 10 segments. The problem has 28 design variables consisting of 8 ground track variables and 20 parameters defining the vertical profile. To make a fair comparison for the reference case, a composite objective of awakenings and fuel burn with an equal weight vector of [0.5 0.5] is used for optimizing the vertical profiles.

The Pareto-optimal solutions obtained by both methods are illustrated in Figure 8, and the ground tracks are provided in Figure 9. To acquire these results, NSGA-II spends 50,000 model evaluations in 9.92 hours, while MOEA/D converges after 37,331 model evaluations in 7.95 hours. The resulting ground tracks are reasonable. In a comparison with the reference case, it can be seen that most of the optimal cases dominate the reference case.

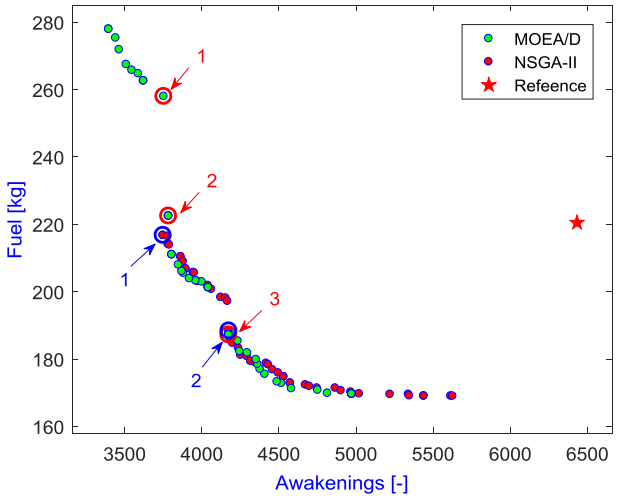

Figure 8. Comparison of Pareto-optimal solutions obtained by NSGA-II and MOEA/D and the result of the reference case.

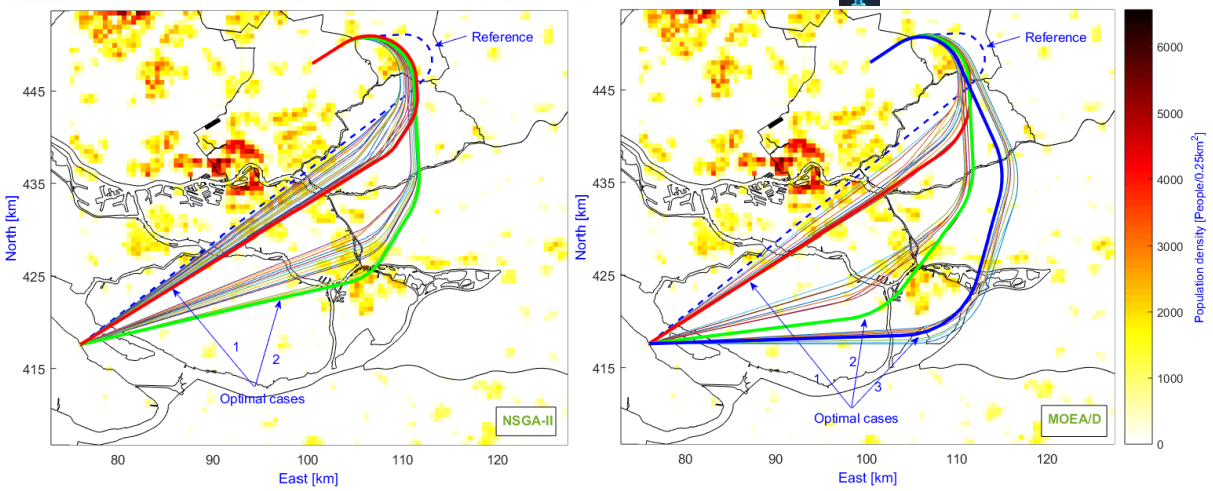

Figure 9. Optimal ground tracks obtained by NSGA-II and MOEA/D.

For a comparison of specific values, the number of awakenings and fuel burn of the representative cases extracted from the Pareto-solution solutions (as numbered in Figure 8) are presented Table 2. Their vertical profiles are provided in Figure 10. It seems that even the ground track of the reference case is shorter than cases 2 of MOEA/D and NSGA-II; its flight time is still higher though. This can be due to the trade-off of two objectives of fuel burn and awakenings with an equal priority.

Table 2. Comparison of objectives of the representative cases and the reference case.

Case no.		Time (s)	Fuel (kg)	Awakening
Reference		570.09	220.49	6432
1	MOEA/D	489.64	187.19	4175
	NSGA-II	480.47	188.39	4176
2	MOEA/D	530.02	222.48	3785
	NSGA-II	527.43	216.74	3749
3	MOEA/D	594.03	257.98	3754

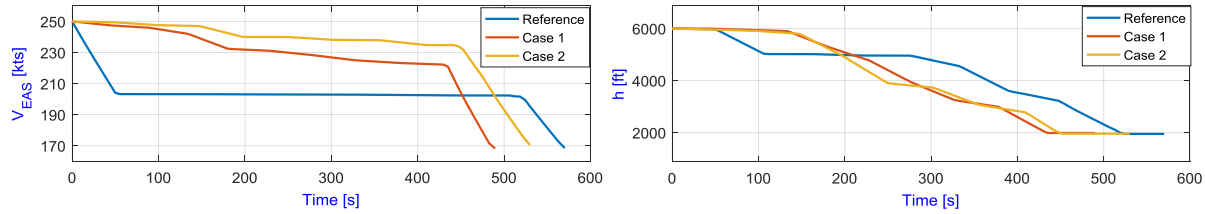

Figure 10. Vertical profiles of cases 1 and 2 and the reference case.

Summarily, based on the obtained results, it can be concluded that MOEA/D is an effective method for handling the optimal design of noise abatement terminal routes. Compared to NSGA-II, MOEA/D generally outperforms NSGA-II in terms of both the quality of solutions and computation time.

7 CONCLUSION

In this paper, a new application of a well-known method named MOEA/D for solving the optimization problems of noise abatement terminal routes is presented. In MOEA/D, besides its typical advantages, its performance is also improved significantly by the integration of new features recently developed, which consist of an adaptive replacement strategy, a stopping condition criterion and a constraint-handling technique. The applicability and effectiveness of MOEA/D are demonstrated through two example scenarios related to Rotterdam The Hague Airport, including a standard instrument departure route, i.e. WOODY1B and a standard terminal arrival route, i.e. STD. The results obtained by MOEA/D are also compared to those of NSGA-II. The comparative results reveal that MOEA/D is generally better than NSGA-II in both the quality of solutions and the convergence rate, and hence it is an adequate algorithm for solving these kinds of problems.

In future work, MOEA/D will be extended for different routes at other airports, and its performance will also be investigated in different problems like route and runway allocations. Furthermore, the

performance of the algorithm will also be enhanced further to deal with large and complex problems, especially in the distribution of solutions and the convergence rate.

REFERENCES

[1] "http://abbb.studioadev.net/economic-growth/beyond-today. (accessed 12 July 2017)."
[2] H. G. Visser and R. a. A. Wijnen, "Optimization of Noise Abatement Departure Trajectories," *J. Aircr.*, vol. 38, no. 4, pp. 620–627, 2001.
[3] S. Hartjes, H. G. Visser, and S. J. Hebly, "Optimisation of RNAV noise and emission abatement standard instrument departures," *Aeronaut. J.*, vol. 114, no. 1162, pp. 757–767, 2010.
[4] R. H. Hogenhuis, S. J. Hebly, and H. G. Visser, "Optimization of area navigation noise abatement approach trajectories," *Proc. Inst. Mech. Eng. Part G-Journal Aerosp. Eng.*, vol. 225, no. G5, pp. 513–521, 2011.
[5] M. L. Braakenburg, S. Hartjes, and H. G. Visser, "Development of a Multi-Event Trajectory Optimization Tool for Noise-Optimized Approach Route Design," *AIAA J.*, no. September, pp. 1–13, 2011.
[6] X. Prats, V. Puig, J. Quevedo, and F. Nejjari, "Lexicographic optimisation for optimal departure aircraft trajectories," *Aerosp. Sci. Technol.*, vol. 14, no. 1, pp. 26–37, 2010.
[7] X. Prats, V. Puig, J. Quevedo, and F. Nejjari, "Multi-objective optimisation for aircraft departure trajectories minimising noise annoyance," *Transp. Res. Part C Emerg. Technol.*, vol. 18, no. 6, pp. 975–989, 2010.
[8] R. Torres, J. Chaptal, C. Bès, and J.-B. Hiriart-Urruty, "Optimal , Environmentally Friendly Departure Procedures for Civil Aircraft," *J. Aircr.*, vol. 48, no. 1, pp. 11–23, 2011.
[9] S. Hartjes and H. Visser, "Efficient trajectory parameterization for environmental optimization of departure flight paths using a genetic algorithm," *Proc. Inst. Mech. Eng. Part G J. Aerosp. Eng.*, vol. 0, no. 0, pp. 1–9, 2016.
[10] H. Li and Q. Zhang, "Multiobjective Optimization Problems With Complicated Pareto Sets, MOEA/D and NSGA-II," *IEEE Trans. Evol. Comput.*, vol. 13, no. 2, pp. 284–302, 2009.
[11] Z. Wang, Q. Zhang, A. Zhou, M. Gong, and L. Jiao, "Adaptive Replacement Strategies for MOEA/D," *IEEE Trans. Cybern.*, vol. 46, no. 2, pp. 474–486, 2016.
[12] K. M. Abdul Kadhar and S. Baskar, "A stopping criterion for decomposition-based multi-objective evolutionary algorithms," *Soft Comput.*, pp. 1–20, 2016.
[13] M. A. Jan and R. A. Khanum, "A study of two penalty-parameterless constraint handling techniques in the framework of MOEA/D," *Appl. Soft Comput. J.*, vol. 13, no. 1, pp. 128–148, 2013.
[14] "International Civil Aviation Organization. Procedures for air navigation services – Aircraft operations. Vol. I, Flight Procedures, ICAO document number 8168, 2006."
[15] "Federal Interagency Committee on Aviation Noise. Effects of aviation noise on awakenings from sleep. March 1997."
[16] Q. Zhang and H. Li, "MOEA/D: A Multiobjective Evolutionary Algorithm Based on Decomposition," *IEEE Trans. Evol. Comput.*, vol. 11, no. 6, pp. 712–731, 2007.
[17] A. Trivedi, D. Srinivasan, K. Sanyal, and A. Ghosh, "A Survey of Multiobjective Evolutionary Algorithms based on Decomposition," *IEEE Trans. Evol. Comput.*, no. c, pp. 1–1, 2016.
[18] P. P. Biswas, R. Mallipeddi, P. N. Suganthan, and G. A. J. Amaratunga, "A multiobjective approach for optimal placement and sizing of distributed generators and capacitors in distribution network," *Appl. Soft Comput.*
[19] A. Konstantinidis and K. Yang, "Multi-objective energy-efficient dense deployment in Wireless Sensor Networks using a hybrid problem-specific MOEA/D," *Appl. Soft Comput. J.*, vol. 12, no. 7, pp. 1847–1864, 2012.
[20] Q. Zhang, W. Liu, and H. Li, "The performance of a new version of MOEA/D on CEC09 unconstrained MOP test instances," *2009 IEEE Congress on Evolutionary Computation*. pp. 203–208, 2009.
[21] M. Xue and S. Zelinski, "Integrated Arrival- and Departure-Schedule Optimization Under Uncertainty," *J. Aircr.*, vol. 52, no. 5, pp. 1437–1443, 2015.
[22] K. Deb, S. Pratab, S. Agarwal, and T. Meyarivan, "A Fast and Elitist Multiobjective Genetic Algorithm: NGSA-II," *IEEE Trans. Evol. Comput.*, vol. 6, no. 2, pp. 182–197, 2002.